Composite Materials with Viscoelastic Stiffness Greater Than Diamond

T. Jaglinski,[1] D. Kochmann,[2] D. Stone,[3] R. S. Lakes[4]*

We show that composite materials can exhibit a viscoelastic modulus (Young's modulus) that is far greater than that of either constituent. The modulus, but not the strength, of the composite was observed to be substantially greater than that of diamond. These composites contain barium-titanate inclusions, which undergo a volume-change phase transformation if they are not constrained. In the composite, the inclusions are partially constrained by the surrounding metal matrix. The constraint stabilizes the negative bulk modulus (inverse compressibility) of the inclusions. This negative modulus arises from stored elastic energy in the inclusions, in contrast to periodic composite metamaterials that exhibit negative refraction by inertial resonant effects. Conventional composites with positive-stiffness constituents have aggregate properties bounded by a weighted average of constituent properties; their modulus cannot exceed that of the stiffest constituent.

In most elastic systems, a deformed object experiences a force with a component in the same direction as the deformation, so that the stiffness is positive. Negative structural stiffness (i.e., force/displacement ratio) can occur in prestrained objects such as tubes buckled to form kinks, which contain stored energy at equilibrium (*1*). Experimentally, negative structural stiffness has been observed in lumped buckled systems composed of rubber tubes (*2*) and models of single foam cells (*3*).

The elastic modulus, a stress/strain ratio, is a measure of material stiffness. A negative modulus is anticipated in the context of Landau's (*4*) theory of phase transformation. As the temperature T is lowered from a value above the transformation temperature, an energy function of both strain ε and temperature (Fig. 1) with a single minimum gradually flattens, then develops two minima or potential wells. If the strain is a shear strain, the transformation is martensitic; for a hydrostatic strain, it is a volume-change transformation. The curvature of this energy function represents an elastic modulus, so that the flattening of the curve corresponds to a softening of the modulus near a critical temperature T_c, a phenomenon observed experimentally. Below T_c, the reversed curvature at a small strain represents a negative modulus. A negative modulus, in which the force that deforms an object is in the direction opposite to the displacement, is distinct from a negative Poisson's ratio, in which a material expands laterally when it is stretched (*5*–*7*). A negative modulus may occur in a predeformed object; it is then a negative incremental modulus. An object with all free surfaces and a negative modulus is unstable. A negative shear modulus causes bands or domains to form, even if the surfaces are constrained. A solid object with a negative bulk modulus (inverse compressibility) can be stabilized by a constraint of the surfaces (*8*), in contrast to fluids (*9*). Negative incremental compressibility has been observed in small-cell foams (*10*). Negative compressibility differs from negative thermal expansion (*11*), which is the stable contraction of an unconstrained object because of a temperature increase.

Negative stiffness can give rise to extreme values of physical properties in heterogeneous systems. For example, both negative stiffness and the resulting giant damping were observed (*2*) in a lumped system containing discrete buckled tubes. A composite with negative-stiffness inclusions is predicted to give rise to material properties greater than those of either constituent (*12*, *13*). Such behavior exceeds classical bounds (*14*), in which composite properties cannot exceed the properties of the constituents. These bounds are theorems assuming that each constituent initially contains no stored energy. Negative stiffness entails initial stored energy; viscoelastic dissipation, if present, enhances composite stability. In composites (*15*), anomalous high viscoelastic damping was observed and attributed to a negative shear modulus in ferroelastic inclusions that were partially constrained by the matrix. These inclusions were sufficiently small that some of them were single domains. Similar composites (*16*) of higher concentration exhibited instability, as predicted by a composite theory incorporating a negative shear modulus.

Composite materials were prepared with inclusions of barium titanate ($BaTiO_3$) in a tin matrix. $BaTiO_3$ was used because it is a ferroelastic, and also a ferroelectric, solid that exhibits a crystal volume change and a crystal shape change during phase transformations, specifically cubic-to-tetragonal transformations at T_c near 120°C and tetragonal-to-orthorhombic transformations near 5°C. The rationale for considering this class of phase transformation is that we can have a negative bulk modulus K in a constrained inclusion and yet still have stability. Constraint by the matrix restrains the transformation over a range of temperatures. Inclusions were, by design, sufficiently large to contain many domains below T_c. The bulk modulus of a material affects its stiffness in bending but not in torsion, because bending entails a local volume change.

Polycrystalline $BaTiO_3$ was fragmented and sieved to achieve a particle-size distribution between 210 and 150 μm. Domains in such materials can be smaller than 1 μm. Some particles were plated with nickel to improve their interface quality. Composites were fabricated using plated or unplated particles of the same pre-plated sizes. Dispersion of particle inclusions was achieved through an ultrasonic casting technique (*17*). Specimens (*18*) were sectioned from ingots, by means of a low-speed diamond saw, into rectangular

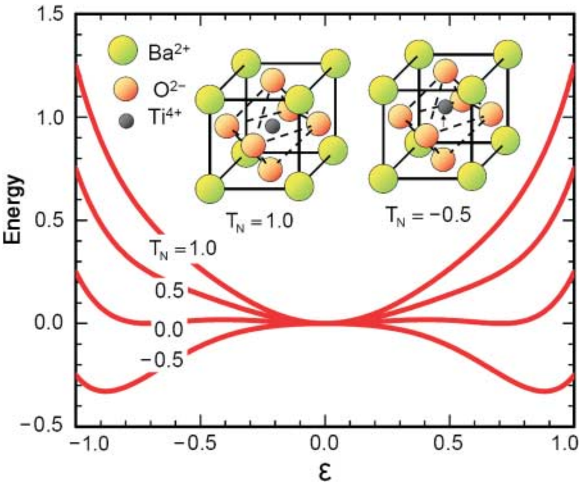

Fig. 1. Landau energy function (*18*) of strain ε and normalized temperature $T_N = (\alpha\gamma/\beta^2)(T - T_1) - 0.25$, with unit cells of $BaTiO_3$ in cubic and tetragonal phases. α, γ, and β are constants that depend on the material.

---

[1] Institute of Shock Physics, Washington State University, Pullman, WA 99163, USA. [2] Institute of Mechanics, Ruhr-University Bochum, 44780 Bochum, Germany. [3] Department of Materials Science, University of Wisconsin–Madison, 541 Engineering Research Building, 1500 Engineering Drive, Madison, WI 53706–1687, USA. [4] Department of Engineering Physics, University of Wisconsin–Madison, 541 Engineering Research Building, 1500 Engineering Drive, Madison, WI 53706–1687, USA.

*To whom correspondence should be addressed. E-mail: lakes@engr.wisc.edu

cross sections, typically 2 mm × 2 mm × 3.5 cm, or they were cut into cylinders with diameters of 2.6 mm and lengths of 3 cm, by means of a wire electric-discharge milling machine. Digital optical micrographs of polished composite specimens were taken. Specimens were tested in bending by means of broadband viscoelastic spectroscopy (*19*). This instrument, which is capable of isothermal internal friction studies over 11 orders of magnitude in frequency, was modified to allow operation up to 300°C and to detect spontaneous strain exceeding 10^{-4}. The viscoelastic response was measured at 100 Hz in bending, which is well below any natural frequency. Torque was applied electromagnetically, and deformation was measured by a laser method. Temperature was monitored with a thermocouple in the air flow within 1 mm of the specimen, so as to avoid interference with viscoelastic measurement. Heating and cooling rates were 0.05 to 0.5°C/s. The procedure is typical of viscoelastic studies of materials, including those that undergo transformation.

Of the 13 specimens with plated inclusions, all exhibited an anomalous viscoelastic response in bending. An anomalous response is defined as a change in modulus or damping that is larger than could be accounted for by composite theory (*20*), assuming a positive inclusion modulus of any value between zero and infinity. Three specimens exhibited large anomalies and three exhibited a Young's modulus ($|E^*|$, absolute value of the complex viscoelastic modulus) greater than that of diamond. Because all materials exhibit some damping, any measured modulus is a viscoelastic modulus. Of the 15 specimens with unplated inclusions, 11 exhibited an anomalous response, and 1 exhibited a Young's modulus greater than that of diamond. It is theorized that the degree of the anomalous response depends on the quality of the inclusion/matrix interface. No anomalous behavior was observed in torsion. The microstructure of a specimen from the latter series, with inclusions measuring 10% by volume, is shown in Fig. 2. Modulus and damping (tan δ, with δ representing the phase between stress and strain) of this specimen are shown in Fig. 3. Given the modest damping, the magnitude of the modulus $|E^*|$ exceeds the real part E' by only about 2%. Young's modulus exceeds that of diamond over a narrow range of temperatures. Transient negative viscoelastic damping (tan δ) indicates the release of stored energy from the inclusions. Although they are stiff, these materials are not expected to be unusually strong or hard. Negative specific heat was observed in those specimens that exhibited the largest mechanical effects (*18*). This behavior is consistent with the negative bulk moduli of the inclusions because the theoretical specific heat depends on the constituent bulk moduli (*21*).

The behavior of all composites changed with thermal cycling, as was also observed in composites (*16*) with VO_2 inclusions; peaks tended to shift to higher temperatures and to attenuate with cycling. Composites with plated inclusions maintained their behavior over a greater number of cycles than did materials in which the inclusions were not plated. The inclusion/matrix interface is therefore clearly important in determining the behavior of the composites. Extreme elastic anomalies were observed for as many as five cycles in a particular specimen. Composite analysis (*13*) shows that macroscopic strain can be magnified locally by several orders of magnitude in the vicinity of the inclusions during the phase transformation. The macroscopic strain amplitude (less than 4×10^{-6} in these experiments) can therefore give rise to a local strain that is sufficient to cause yield in the tin matrix. This amplified local strain can account for the cycle dependence that could be ameliorated by using a stronger matrix.

Broad peaks in damping (tan δ) were also observed, as shown in Fig. 4. Even modest effects in these composites are notable because for a dilute particulate morphology, composite properties are known (*14*, *20*) to be relatively insen-

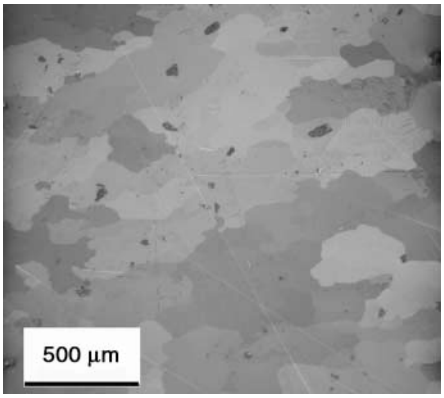

Fig. 2. Cross section of composite specimen in polarized light. $BaTiO_3$ inclusions appear as black spots. The polycrystalline structure of the tin matrix is shown in grayscale. Scale bar, 500 μm.

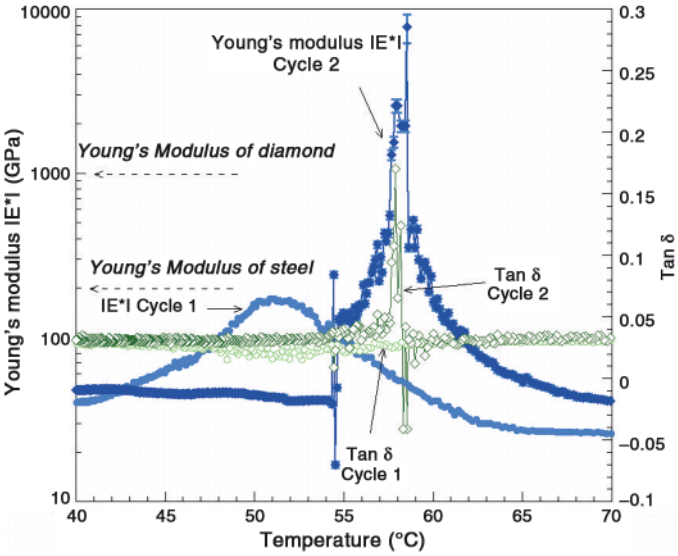

Fig. 3. Young's modulus $|E^*|$ and viscoelastic damping tan δ of the composite in Fig. 2, showing extremely high modulus over a range of temperatures. δ is the phase angle between stress and strain. Young's moduli of the constituents are $BaTiO_3$, 100 GPa; and tin, 50 GPa. Error bars (4%, smaller than data points) in the low-modulus regime are dominated by irregularity in the specimen diameter and in the high-modulus regime are dominated by digital resolution of the lock-in amplifier. Errors in tan δ, ~0.001, are smaller than the data points.

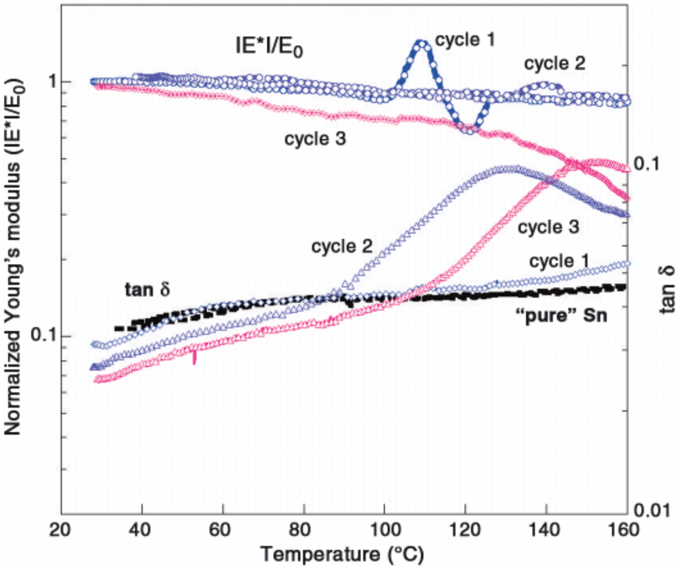

Fig. 4. Broad peaks in Young's modulus and viscoelastic damping (tan δ) of a composite similar to that in Fig. 2. E_0 is the normalizing modulus, which has a value of 30 GPa.

sitive to inclusion properties when they have a positive modulus. For example, with a 10% concentration of particles, the composite modulus $|E^*|$ due to infinitely stiff inclusions is predicted to increase by 22% as compared with that of the pure matrix. The composite damping due to inclusions with a peak damping tan $\delta = 0.06$, corresponding to bulk $BaTiO_3$, is predicted to be only 6% greater than that of the matrix. The damping peaks shown in Fig. 4 (8% inclusion concentration) correspond to a factor of 2 increase as compared with pure tin (also shown), so, as with the above giant anomalies in the modulus, negative compressibility of the inclusions is inferred.

The present extreme-stiffness results are based on negative compressibility (inverse bulk modulus K, resistance to volume change) of inclusions, in contrast to the negative shear modulus G (resistance to shape change) in earlier Sn-VO_2 composites (*15*) that exhibited large damping but modest (5%) anomalies in the modulus. These three-dimensional aspects of deformation govern the stability and properties of materials. Positive values of G and K give rise to a positive-definite strain energy and hence to the stability of an object with free surfaces and no constraint. This corresponds to the usual allowable range of Poisson's ratio ν, $-1 < \nu < 0.5$, allowing a negative Poisson's ratio in isotropic solids (*5*). For the less restrictive condition of strong ellipticity, which entails real positive velocities of shear and longitudinal waves, $G > 0$ and $-4G/3 < K < \infty$. A strongly elliptic solid constrained at the surface is incrementally stable (*22*) and has a unique elasticity solution (*23*), so a range of negative bulk modulus is allowed. A material with negative shear modulus G is unstable with respect to domain formation. Surface energy limits how small a domain can be, so a sufficiently small crystal can be a single domain and can operate as a negative-stiffness inclusion, as was the case in Sn-VO_2 composites. There is no such inclusion size limitation associated with a negative bulk modulus. An inclusion in a composite is under partial constraint.

Diamond has long been considered to have maximal properties such as stiffness and hardness. The achievement of substantially greater stiffness illustrates the importance of composites with negative-stiffness inclusions. These composites have potential in high-performance materials in which high stiffness or high dissipation are of use. They may occur naturally in rocks and play a role in deep-focus earthquakes.

References and Notes

1. J. M. T. Thompson, *Philos. Trans. R. Soc. London Ser. A* **292**, 1 (1979).
2. R. S. Lakes, *Philos. Mag. Lett.* **81**, 95 (2001).
3. R. S. Lakes, P. Rosakis, A. Ruina, *J. Mater. Sci.* **28**, 4667 (1993).
4. L. D. Landau, in *Collected Papers of L. D. Landau*, D. Ter Taar, Ed. (Gordon and Breach/Pergamon, New York, 1965), pp. 193–216.
5. R. Lakes, *Science* **235**, 1038 (1987).
6. A. Yeganeh-Haeri, D. J. Weidner, J. B. Parise, *Science* **257**, 650 (1992).
7. R. H. Baughman, J. M. Shacklette, A. A. Zakhidov, S. Stafstrom, *Nature* **392**, 362 (1998).
8. Within continuum mechanics, there is no size limitation for a constrained object of negative bulk modulus to be stable. Thermodynamics suggests a size-dependent metastability associated with negative compressibility, owing to the nonzero size of atoms and the nonzero temperature. The time scale for such metastability in solids may, however, exceed experimental time scales. Indeed, diamond itself is metastable.
9. J. Van der Waals, thesis, University of Leiden, Netherlands (1873) [English translation, J. R. Rowlinson, Ed. (North Holland, Amsterdam, 1988)].
10. B. Moore, T. Jaglinski, D. S. Stone, R. S. Lakes, *Philos. Mag. Lett.* **86**, 651 (2006).
11. T. A. Mary, J. S. O. Evans, T. Vogt, A. W. Sleight, *Science* **272**, 90 (1996).
12. R. S. Lakes, *Phys. Rev. Lett.* **86**, 2897 (2001).
13. R. S. Lakes, W. J. Drugan, *J. Mech. Phys. Solids* **50**, 979 (2002).
14. Z. Hashin, S. Shtrikman, *J. Mech. Phys. Solids* **11**, 127 (1963).
15. R. S. Lakes, T. Lee, A. Bersie, Y. C. Wang, *Nature* **410**, 565 (2001).
16. T. Jaglinski, R. S. Lakes, *Philos. Mag. Lett.* **84**, 803 (2004).
17. Y. Yang, J. Lan, X. Li, *Mater. Sci. Eng. A* **380**, 378 (2004).
18. Materials and methods are available as supporting material on *Science* Online.
19. T. Lee, R. S. Lakes, A. Lal, *Rev. Sci. Instrum.* **71**, 2855 (2000).
20. Z. Hashin, *J. Appl. Mech.* **29**, 143 (1962).
21. B. W. Rosen, Z. Hashin, *Int. J. Eng. Sci.* **8**, 157 (1970).
22. Lord Kelvin (Thomson, W.), *Philos. Mag.* **26**, 414 (1888).
23. E. Cosserat, F. Cosserat, *C. R. Acad. Sci. Paris* **126**, 1089 (1898).

24. Partial support by NSF and by the NSF Materials Research Science and Engineering Center program is gratefully acknowledged. We thank W. Drugan for stimulating discussions.

Supporting Online Material

www.sciencemag.org/cgi/content/full/315/5812/620/DC1
Materials and Methods
References

3 October 2006; accepted 12 December 2006
10.1126/science.1135837

Coupling Coherence Distinguishes Structure Sensitivity in Protein Electron Transfer

Tatiana R. Prytkova, Igor V. Kurnikov,* David N. Beratan†

Quantum mechanical analysis of electron tunneling in nine thermally fluctuating cytochrome b_{562} derivatives reveals two distinct protein-mediated coupling limits. A structure-insensitive regime arises for redox partners coupled through dynamically averaged multiple-coupling pathways (in seven of the nine derivatives) where heme-edge coupling leads to the multiple-pathway regime. A structure-dependent limit governs redox partners coupled through a dominant pathway (in two of the nine derivatives) where axial-ligand coupling generates the single-pathway limit and slower rates. This two-regime paradigm provides a unified description of electron transfer rates in 26 ruthenium-modified heme and blue-copper proteins, as well as in numerous photosynthetic proteins.

Many biological pathways depend on the facilitation of electron transfer (ET) processes by proteins (*1–14*). At the simplest level, this acceleration in rate can be explained by empirical models that omit the details of protein structure and describe the fact that proteins lower the barrier to electron tunneling by about 3 eV relative to that of vacuum tunneling (*1*, *14*). However, ET rates can be slower or faster in different proteins, despite the electron's traveling a similar distance between donors and acceptors (R_{DA}) (*1–3*). These rate differences can arise because tunneling is faster through covalent bonds than through weak or nonbonded contacts (*10*), and the composition of the coupling medium between donor and acceptor varies with the primary, secondary, and tertiary structure of the protein (*1*, *2*, *10*).

The simplest model that accounts for such structural effects on ET rates is the pathway model (*10*), which identifies the most facile coupling routes between the donor and acceptor. Packing-density models analyze atom density between the donor and acceptor. The predictions of the pathway and packing-density models are nearly the same (*4*, *15*). Nonetheless, there are many examples where an even simpler exponential model (*14*)

$$k_{ET} \propto \exp[-\beta R_{DA}] \qquad (1)$$

, where k_{ET} is the ET rate and β is an exponential decay constant, can account for the observed ET rates without including three-dimensional details of protein structure.

The limits of validity for these simple tunneling models have been poorly understood, and understanding has been further hampered by the lack of sufficiently detailed data sets on ET rates for the same protein that would allow for meaningful comparisons; in comparing ET rates between different proteins, it is difficult to separate the electron-tunneling factors from the nuclear factors, or Marcus factors (*16*), that arise in the ET theory (*1*, *2*). We have now analyzed a recent set of tunneling-limited ET rates obtained by Winkler and Gray for a Ru-modified heme protein [cytochrome (cyt) b_{562}]. The exponential distance-decay model accounts for some but not

---

Departments of Chemistry and Biochemistry, Duke University, Durham, NC 27708, USA.

*Present address: Department of Environmental and Occupational Health, University of Pittsburgh, Pittsburgh, PA 15219–3130, USA.

†To whom correspondence should be addressed. E-mail: david.beratan@duke.edu